

Using molecular similarity to construct accurate semiempirical electronic structure theories

Benjamin G. Janesko and David Yaron*

Department of Chemistry, Carnegie Mellon University, Pittsburgh, PA 15213

A methodology is developed for building semiempirical exchange-correlation functionals for large molecules. The method uses molecular similarity by assuming that data collected for a molecular subsystem in various environments, such as for an aldehyde functional group in different molecules and electrostatic fields, contains the information needed to describe it in other similar environments. The method uses a data set of highly accurate calculations on a molecular subsystem to map the subsystem two-electron density onto its one-electron density. The two-electron density, and therefore the exchange-correlation functional, of a large molecule is approximated from the predicted two-electron densities of overlapping molecular subsystems. The method is demonstrated on two simple model systems: full inclusion of correlation on minimal-basis hydrogen chains and MP2 on substituted aldehydes.

*Electronic address: yaron@cmu.edu

Canonical *ab initio* electronic structure methods provide highly accurate electronic structures for small systems of $\mathcal{O}(10)$ atoms. However, the computational effort of these methods scales poorly with system size, requiring up to exponential scaling for the exact, fully-correlated solution in a given basis set. There has been much progress over the last several years in developing *ab initio* methods that can accurately treat electron correlation with reduced computational effort [1, 2, 3]. While these methods are useful, their computational expense still precludes their application to large systems such as proteins.

Semiempirical electronic structure theories [4, 5] provide a route to modeling systems that are too large for *ab initio* treatment. Here we develop accurate semiempirical methods for treating electron correlation. These methods construct the electronic structures of large systems by (i) extracting information from rich data sets of *ab initio* calculations on small systems, and (ii) combining this information using the assumptions of nearsightedness and molecular similarity.

Nearsightedness, as put forth in Ref. [6], is the principle that a many-electron system's local electronic structure about a point \mathbf{r} is largely determined by the effective potential for points \mathbf{r}' *near* \mathbf{r} . Molecular similarity is simply the idea that molecular subsystems (-CH₃, -OH, etc.) behave roughly the same way in different molecules. The assumption of nearsightedness can be implemented in any theory (semiempirical or *ab initio*) that represents electronic structure in terms of local information, such as electron densities [7, 8, 9] or correlations between localized orbitals [3, 10, 11]. The assumption of molecular similarity is at the heart of chemistry, and underlies the atom- or functional-group-specific parameters of semiempirical theories.

We implement a nearsighted treatment of electron correlation by representing electronic structure in terms of one- and two-electron densities. A system's one- and two-electron density matrices 1D , 2D are obtained from its normalized N -electron wavefunction $|\Phi\rangle$ as

$${}^1D_b^a = \langle \Phi | a_a^\dagger a_b | \Phi \rangle \quad (1)$$

$${}^2D_{ac}^{bd} = 1/2 \langle \Phi | a_b^\dagger a_d^\dagger a_a a_c | \Phi \rangle \quad (2)$$

in second quantization with one-electron basis functions $\{|a\rangle\}$. The electron density in real space is the diagonal of the one-electron density matrix: ${}^1D(\mathbf{r}) \equiv \langle \Phi | a_\mathbf{r}^\dagger a_\mathbf{r} | \Phi \rangle$ [12]. 1D and 2D provide a complete description of a system whose Hamiltonian contains only one- and two-body interactions [13].

The two-electron density 2D obtained from $|\Phi\rangle$ can be expressed as a cumulant expansion [14, 15]

$$\begin{aligned} {}^2D_{bd}^{ac} &= 1/2 {}^1D_a^b {}^1D_c^d - ({}^2D_X)_{bd}^{ac} + {}^2\Delta_{bd}^{ac} \\ ({}^2D_X)_{bd}^{ac} &\equiv 1/2 {}^1D_d^a {}^1D_c^b \end{aligned} \quad (3)$$

where the three terms on the right-hand side of Eq. 3 are denoted Coulomb, exchange, and correlation contributions to 2D and the connected pair density ${}^2\Delta$ cannot be written as a simple function of 1D .

The Coulomb and exchange contributions to 2D in Eq. 3 are well-approximated at the Hartree and Hartree-Fock levels of theory, respectively. However, accurate *ab initio* treatment of the connected pair density ${}^2\Delta$ requires expensive high-level methods. Nearsightedness suggests that a large system's ${}^2\Delta$ can be assembled, as described in Ref. [6] and schematized in Fig. 1, by (i) partitioning the system into $\mathcal{O}(N)$ overlapping subsystems, (ii) independently evaluating each subsystem ${}^2\Delta$, and (iii) assembling the subsystem results into a ${}^2\Delta$ for the entire system. The resulting system ${}^2\Delta(\mathbf{r}, \mathbf{r}')$ is accurate for length scales $|\mathbf{r} - \mathbf{r}'|$ up to the order of subsystem size. This non-variational method for assembling ${}^2\Delta$ is similar in spirit to localized coupled-cluster [3, 16, 17, 18] and divide-and-conquer theories [7, 8, 9]. Our “localized reduced density matrix” (LRDM) approach [19] assembles ${}^2\Delta$ from *ab initio* subsystem calculations in an atomic orbital basis set [20].

The LRDM method schematized in Fig. 1 provides a route to implementing semiempirical, molecular-similarity based approximations for ${}^2\Delta$. We use highly accurate *ab initio* calculations to construct databases of a molecular subsystem's ${}^2\Delta$ in different environments. The information in these databases can be “mined” to parametrize functionals that return the subsystem's ${}^2\Delta$ as a function of simple characteristics of the subsystem and its environment (e.g. subsystem geometry, subsystem 1D , environment multipole moments). The predicted ${}^2\Delta$ for all of a molecule's subsystems are combined as in LRDM to give a semiempirical approximation for ${}^2\Delta$ of the entire system.

In the current work, we parametrize functionals that predict subsystem ${}^2\Delta$ or ${}^2D_{XC}$ as a function of subsystem one-electron density 1D . (We will use ${}^2D[{}^1D]$ as a generic term for functionals that return a molecular subsystem's ${}^2\Delta$ or ${}^2D_{XC}$ as a functional of its 1D .) The functionals are used as correlation or exchange-correlation functionals in density functional theory, as described below. The proposed method may also be useful for density matrix functional theory [21].

Density functional theory (DFT) is a formally exact method for treating a system of N interacting electrons in terms of the one-electron density of a system of noninteracting electrons [13, 22, 23]. The electron-electron interaction

energy is treated as the sum of a mean-field Coulomb term and an exchange-correlation correction E_{XC} , such that the electrons move in a one-electron potential corrected by $v_{XC}(\mathbf{r}) = \delta(E_{XC})/\delta(^1D(\mathbf{r}))$. DFT is implemented by approximating v_{XC} as a functional of electron density: $v_{XC} = v_{XC}[^1D]$. The exchange-correlation energy E_{XC} may be obtained as the trace over the exchange-correlation two-electron density: $E_{XC} = \sum \langle ac|bd \rangle (^2D_X + ^2\Delta)_{ac}^{bd}$. Thus, a system's exchange-correlation functional $v_{XC}[^1D]$ or its correlation component $v_{corr}[^1D]$ can be obtained from the first derivative of the system's $^2D_{XC}[^1D]$ or $^2\Delta[1D]$ functional, respectively (see Eq. 5).

We fit subsystem $^2\Delta[1D]$ and $^2D_{XC}[^1D]$ functionals to a truncated Taylor expansion and use principle component analysis of the training set densities in the atomic orbital basis. For example, matrix elements of a functional of the connected pair density $^2\Delta[1D]$ are fit as

$$(^2\Delta[1D])_{ac}^{bd} = \sum_j \left\{ (^2\Delta_j)_{ac}^{bd} \right. \\ \left. \times \sum_i \gamma_{ij} \langle ^1D | ^1D_i \rangle + \sigma_{ij} (\langle ^1D | ^1D_i \rangle)^2 \right\} \quad (4)$$

where $\{|^2\Delta_i\rangle\}$ and $\{|^1D_i\rangle\}$ are density matrix principle components, $\langle ^1D | ^1D_i \rangle$ is the projection of the argument one-electron density 1D onto the i th principle component, and $\{\gamma_{ij}, \sigma_{ij}\}$ are fitted parameters [24]. Second-order truncation has a physical basis in that 2D and $^1D \times ^1D$ have the same dimensionality. Matrix elements of a subsystem's correlation energy operator $v_{corr}[^1D]$ are obtained as

$$(v_{corr}[^1D])_{a'}^{b'} = \sum_{abcd} \langle ac|bd \rangle \sum_j \left\{ (^2\Delta_j)_{ac}^{bd} \right. \\ \left. \times \sum_i (\gamma_{ij} + 2\sigma_{ij} \langle ^1D | ^1D_i \rangle) | ^1D_i \rangle_{a'}^{b'} \right\}. \quad (5)$$

The system $v_{corr}[^1D]$ functional is obtained by overlaying subsystem contributions as in LRDM (Fig. 1). These are the lowest-order approximation for $^2D[1D]$ functionals, and we expect that more sophisticated functional forms can give more accurate results.

Our DFT correlation functionals differ considerably from the standard DFT functionals LDA [23, 25] and GGA [26], that model $v_{XC}[^1D]$ as that of a homogeneous electron gas. Other authors have developed both semiempirical [27, 28] and subsystem-based [29, 30] $v_{XC}[^1D]$ functionals, but to our knowledge the current method is unique in combining the assumption of molecular similarity with a nearsighted approximation for the two-electron density.

The remainder of this paper details demonstrations of the method. We use GAMESS for all *ab initio* calculations [31]. We begin by demonstrating $^2D[1D]$ functionals with a dimerized chain of ten minimal-basis hydrogen atoms $(\text{H-H})_5$. This system is small enough that the functionals can be compared to exact (FCI) solutions. RHF+FCI/STO-3G calculations were performed on 300 systems. Each system had a random geometry, and was placed in a random field of point charges [32]. The exact 1D and 2D were partitioned into four overlapping $(\text{H-H})_2$ subsystems as in Fig. 1. One-third of the systems were chosen at random to be the training set, with the remainder being the testing set [33]. The training set data were used to train a $^2\Delta[1D]$ and a $^2D_{XC}[^1D]$ functional for $(\text{H-H})_2$, using Eq. (4) [34].

Figure 2 and Table I show predicted energies for $(\text{H-H})_5$ systems, obtained by using the above functionals to predict 2D of the $(\text{H-H})_2$ subsystems and combining the predictions as in LRDM. Table I also includes results from the individual $(\text{H-H})_2$ subsystem functionals. In Fig. 2 and Table I, results quoted as using $^1D_{EXACT}$ use the 1D of the exact solution. Results quoted as using $^1D_{DFT}$ use the 1D obtained from using the $^2\Delta[1D]$ functionals as the correlation-energy functional (Eq. 5) in DFT with exact exchange. Both $^1D_{EXACT}$ and $^1D_{DFT}$ exhibit high correlation between exact and predicted E_{corr} , but there is a small systematic error in the DFT results. The semiempirical functionals sometimes return E_{corr} (and total energy) below the exact energy, as anticipated for a nonvariational method.

As a point of comparison, Fig. 2 and Table I also show correlation energies obtained with a standard approximate method, RHF+MP2. The mean absolute E_{corr} error from RHF+MP2 is greater than 200 mH, compared to the less than 10 mH error from our $^2D[1D]$ functionals. RHF+MP2 also underestimates the variation in the correlation energy across this data set, obtaining a line of slope 0.19 in the plot of predicted versus exact correlation energies, as compared to the slope near one obtained from our $^2D[1D]$ functionals.

The results obtained here are encouraging. A single $^2D[1D]$ functional, fitted to reproduce 2D components, sufficed to describe both energies and energy derivatives for all four of the $(\text{H-H})_2$ subsystems, in a wide range of molecular geometries and electrostatic environments.

To aid transferability between basis sets, subsystem $^2D[1D]$ functionals can be defined from the electron density $^1D(\mathbf{r}) = \langle \Phi | a_{\mathbf{r}}^\dagger a_{\mathbf{r}} | \Phi \rangle$ evaluated on a Cartesian-space grid. For proof-of-principle purposes, we used the data in Fig. 2 to construct real-space $^2\Delta[1D]$ for a small number of points (36 $^2\Delta(\mathbf{r}_1, \mathbf{r}_2)$) fit to quadratic functions of 17 $^1D(\mathbf{r})$ in

an $(H-H)_2$ subsystem. Again, data from one-third of the $(H-H)_5$ systems was used to train the functional. R^2 values between real and predicted ${}^2\Delta(\mathbf{r}_1, \mathbf{r}_2)$ for $(H-H)_5$ were 0.99 for the training set and 0.97 for the testing set.

We next consider correlation and exchange-correlation functionals for a more realistic subsystem, the aldehyde (HOC) subsystem of HOC-CH₂-X molecules [35]. Since exact solutions for this system are not computationally feasible, ${}^2D[{}^1D]$ functionals were fitted to RHF+MP2/6-31G calculations [35]. We generated two data sets of HOC-CH₂-X in random distributions of point charges, denoted “simple” and “augmented” and with substituents X=H and X={H,O⁻} [36]. ${}^2D[{}^1D]$ functionals were fitted to both simple and augmented data sets, using half the data as training set [37]. The functionals were tested on their respective (simple or augmented) data sets. Functionals were tested for their ability to reproduce the subsystem correlation or exchange-correlation energy, defined as e.g. $E_{corr} = \sum \langle ac|bd \rangle {}^2\Delta_{ac}^{bd}; \{abcd\} \in \text{HOC}$.

We also generated an “extrapolated” test data set consisting of HOC-CH₂-X molecules without electrostatic perturbations and with X = -CH₃, -CFH₂, -CF₃, -CN, -CCH, -CHO, -COCl, -NO₂, -OH, -OCH₃, -O⁻, -CO₂⁻, -NH₃⁺, -F, -Cl, -Li, -Na. The degree of extrapolation can be quantified by calculating the average fraction of 1D that lies along the principle components included in the semiempirical functionals of Eq. (4). The average fraction is always greater than 0.97 for training and testing data sets. It is significantly lower for the extrapolated data, 0.80 (0.87) for the functionals parametrized from the simple (augmented) training set.

The results in Table II show that the aldehyde ${}^2D[{}^1D]$ functionals provide a good description of both training and testing data. The quality of the extrapolation varies among the different molecules. Table II includes extrapolation results for four representative HOC-CH₂-X, showing that (a) the effects of some X groups (CN) are well-described by all of the ${}^2D[{}^1D]$ functionals, (b) some X groups (O⁻, NH₃⁺) are described better by the augmented functionals, and (c) a few X groups (OH) are described equally poorly by all of the functionals, indicating that they require more sophisticated ${}^2D[{}^1D]$ functionals and/or a different training set.

We tested ${}^2\Delta[{}^1D]$ and ${}^2D_{XC}[{}^1D]$ functionals for the aldehyde group in molecules without a “buffer” between the aldehyde and the perturbing substituent, HOC-X. Functionals were fitted as above to data on point-charge-perturbed HOC-H. The functionals gave reasonable predictions for the point-charge-perturbed HOC-H data (average E_{corr} and E_{XC} errors of 8.8 and 87 mH, respectively, for the testing set) but significantly worse extrapolation results. This is likely due to the spatial proximity of fitted (HOC) and perturbing (X) subsystems.

This paper explores an approach for constructing semiempirical theories that include accurate electron-electron correlations. Comparison with exact results for a small model system and approximate (MP2) results for a more realistic system suggests the feasibility of the approach. The results are especially encouraging given the simple, low-order data fitting methods employed. The present approach has the potential to complement *ab initio* treatments of correlation, particularly for accurate calculations on large, modular systems such as proteins.

The authors thank Craig J. Gallek for contributions to extensions to GAMESS for RDM manipulation. This work was supported by the National Science Foundation (CHE0316759). BGJ thanks the NSF for additional support.

[1] S. Goedecker, Rev. Mod. Phys. **71**, 1085 (1999).
 [2] R. J. Bartlett, J. Phys. Chem. **93**, 1697 (1989).
 [3] S. Saebo and P. Pulay, Ann. Rev. Phys. Chem. **44**, 213 (1993).
 [4] E. J. Zoebisch, E. F. Healey, J. J. P. Stewart, and M. J. S. Dewar, JACS **107**, 3902 (1985).
 [5] M. Zerner, Rev. Comp. Chem. **2**, 313 (1991).
 [6] W. Kohn, Phys. Rev. Lett. **76**, 3168 (1996).
 [7] W. Yang, Phys. Rev. Lett. **66**, 1438 (1991).
 [8] T.-S. Lee, D. M. York, and W. Yang, J. Chem. Phys. **105**, 2744 (1996).
 [9] S. L. Dixon and K. M. Merz, Jr., J. Chem. Phys. **104**, 6643 (1996).
 [10] W. Förner, J. Ladik, P. Otto, and J. Cizek, Chem. Phys. **97**, 251 (1985).
 [11] P. Y. Ayala and G. E. Scuseria, J. Chem. Phys. **110**, 3660 (1999).
 [12] The real-space density matrix is evaluated in a basis $\{|\phi_a\rangle\}$ as ${}^1D(\mathbf{r}, \mathbf{r}') = \sum_{ab} \langle \Phi | a_a^\dagger a_b | \Phi \rangle \phi_a(\mathbf{r}) \phi_b(\mathbf{r}')$, and the real-space electron density ${}^1D(\mathbf{r}) = {}^1D(\mathbf{r}, \mathbf{r})$ is evaluated the same way with $\mathbf{r} = \mathbf{r}'$. ${}^1D_a^b = \langle \Phi | a_a^\dagger a_b | \Phi \rangle$ generally has nonzero off-diagonal ($a \neq b$) matrix elements in the nonorthogonal basis sets used in the current work.
 [13] R. G. Parr and W. Yang, *Density-Functional Theory of Atoms and Molecules* (Oxford University Press, New York, 1989).
 [14] D. A. Mazziotti, Phys. Rev. A **60**, 4396 (1999).
 [15] D. A. Mazziotti, Phys. Rev. A **60**, 3618 (1999).
 [16] C. Hampel and H.-J. Werner, J. Chem. Phys. **104**, 6286 (1996).
 [17] G. E. Scuseria and P. Y. Ayala, J. Chem. Phys. **111**, 8330 (1999).
 [18] T. Van Voorhis and M. Head-Gordon, J. Chem. Phys. **117**, 9190 (2002).
 [19] B. G. Janesko and D. Yaron, J. Chem. Phys. **119**, 1320 (2003).

System	Method	$\langle E \text{ error} \rangle$		R^2	
		Train	Test	Train	Test
$(\text{H-H})_2$	$^2\Delta[^1D_{EXACT}]$	2.77	2.08	0.978	0.971
$(\text{H-H})_2$	$^2D_{XC}[^1D_{EXACT}]$	3.38	3.83	0.986	0.964
$(\text{H-H})_5$	$^2\Delta[^1D_{EXACT}]$	5.76	3.96	0.976	0.972
$(\text{H-H})_5$	$^2D_{XC}[^1D_{EXACT}]$	6.32	7.68	0.959	0.920
$(\text{H-H})_5$	$^2\Delta[^1D_{DFT}]$	15.26	12.24	0.948	0.961
$(\text{H-H})_5$	RHF+MP2	218.38	211.08	0.983	0.978

TABLE I: Analysis of correlation ($^2D_{XC}[^1D]$) and exchange-correlation ($^2D_{XC}[^1D]$) functionals for $(\text{H-H})_2$. $\langle E \text{ error} \rangle$ is the mean average error in predicted energies in milli-Hartrees. R^2 is the correlation between real and predicted energies. The one-electron densities $^1D_{EXACT}$ and $^1D_{DFT}$ used as inputs for the $^2D[^1D]$ functionals are obtained, respectively, from RHF+FCI calculations and from using the $^2\Delta[^1D]$ functionals as the correlation-energy functional (Eq. 5) in DFT with exact exchange. RHF+MP2 shows error in correlation energy.

- [20] In LRDM, each part of the large molecule lies in the middle of at least one subsystem. Matrix elements from subsystem edges, where nearsighted edge effects on the subsystem $^2\Delta$ are large, are discarded. Otherwise, estimates of a $^2\Delta$ matrix element that are obtained from multiple subsystem calculations are averaged.
- [21] J. Cioslowski, ed., *Many-Electron Densities and Reduced Density Matrices* (Plenum, New York, 2000).
- [22] P. Hohenberg and W. Kohn, Phys. Rev. **136**, b864 (1964).
- [23] W. Kohn and L. J. Sham, Phys. Rev. **140**, A1133 (1965).
- [24] Each component of the two-electron density is fit independently of the others.
- [25] R. O. Jones and O. Gunnarson, Rev. Mod. Phys. **61**, 689 (1989).
- [26] D. C. Langreth and M. J. Mehl, Phys. Rev. B **28**, 1809 (1983).
- [27] A. D. Becke, J. Chem. Phys. **98**, 5648 (1993).
- [28] D. J. Tozer, V. E. Ingamells, and N. C. Handy, J. Chem. Phys. **105**, 9200 (1996).
- [29] W. Kohn and A. E. Mattsson, Phys. Rev. Lett. **81**, 3487 (1998).
- [30] R. Armiento and A. E. Mattsson, Phys. Rev. B **66**, 165117 (2002).
- [31] M. W. Schmidt et al., J. Comput. Chem. **14**, 1347 (1993).
- [32] Each H-H bond length was randomly set between 0.55 and 1.0 Å. Each $(\text{H-H}) \leftrightarrow (\text{H-H})$ spacing was randomly set between 0.9 and 4.0 Å. Ten point charges ($|\text{charge}| \leq 1$) were randomly distributed in a $6\text{\AA} \times 6\text{\AA} \times (\text{molecule length} + 4\text{\AA})$ box around the molecule, with a minimum charge-proton separation of 1.3 Å.
- [33] Comparison of 100 random choices for training set showed the results are invariant to choice of training set.
- [34] Functionals used 6 1D principle components and 14 $^2\Delta$ or 12 $^2D_{XC}$ principle components.
- [35] HOC-CH₂-X geometries were obtained at the RHF/STO-3G level, with the HOC subsystem constrained to the equilibrium geometry of HOC-CH₂-H.
- [36] Eight point charges were placed around each HOC-CH₂-X, with a minimum charge-atom separation of 1.4 Å. Point charge configurations for HOC-CH₂-X were restricted to subsystem energies of $-0.270 < E_{corr} < -0.248$ mH, $-14.0 < E_{XC} < -13.8$ mH, giving 651 X=H configs, 240 X=O⁻ configs for training/testing E_{corr} functionals and 844 X=H configs, 254 X=O⁻ configs for E_{XC} functionals.
- [37] Simple (augmented) $^2\Delta[^1D]$ functionals used 60 1D , 30 $^2\Delta$ (60 1D , 40 $^2\Delta$) components. Simple (augmented) $^2D_{XC}[^1D]$ functionals used 60 1D , 60 $^2D_{XC}$ (80 1D , 80 $^2D_{XC}$) components.

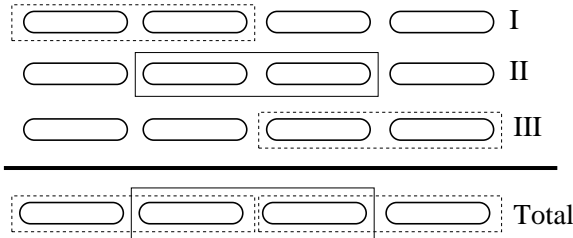


FIG. 1: Schematic of subsystem-based treatment of the two-electron density 2D for a generic four-element chain. 2D for overlapping subsystems (boxed regions) are obtained separately (calculations I-III) and combined into an approximate 2D for the entire system.

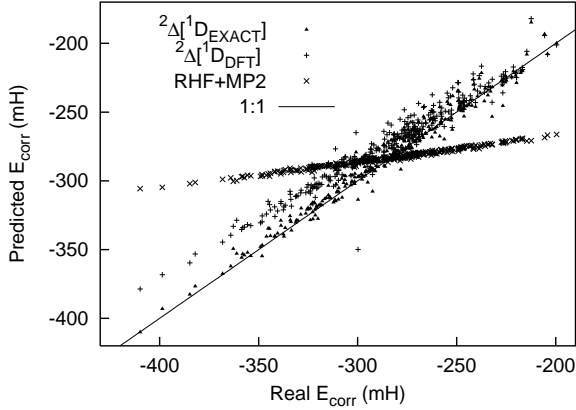


FIG. 2: Real vs. predicted E_{corr} for $(H-H)_5$ systems, with labels as in Table I. RHF+MP2 E_{corr} predictions are shifted by -218.38 mH.

	E_{corr}			E_{XC}			
	δ	simple	aug	δ	simple	aug	RHF
Training	5.05	0.46	0.48	34.83	1.43	1.02	6.04
Testing	4.88	1.12	0.80	33.26	2.78	2.36	5.71
Extrapolated	3.84	1.47	1.37	24.76	7.75	6.63	45.22
CN	3.62	0.22	1.16	14.72	1.76	0.53	34.96
O^-	4.89	5.04	1.02	104.70	27.10	13.20	35.47
NH_3^+	6.23	1.26	0.55	41.96	13.53	9.44	28.57
OH	4.40	1.25	2.03	29.33	17.45	11.52	42.86

TABLE II: Testing functionals for $^2\Delta$ and $^2D_{XC}$ of the HOC subsystem in point-charge-perturbed RHF+MP2/6-31G HOC-CH₂-X. δ is the subsystem's energy change (mH) vs. unperturbed HOC-CH₂-H. Simple and aug are subsystem energy errors for functionals trained on X=H or X={H,O⁻} data sets (see text). RHF is the subsystem E_{XC} error predicted by RHF with a constant correction of -252 mH, the average RHF E_{XC} error for the simple training set. The first three rows are mean absolute errors for training, testing, and extrapolated data. Remaining rows are representative extrapolations for X={CN,O⁻,NH₃⁺,OH}.